JOURNAL OF AGRICULTURAL AND FOOD CHEMISTRY

Article

pubs.acs.org/JAFC

# Co-treatment with Quercetin and 1,2,3,4,6-Penta-*O*-galloyl-*β*-D-glucose Causes Cell Cycle Arrest and Apoptosis in Human Breast Cancer MDA-MB-231 and AU565 Cells

Cheng Huang,[†] Suz-Yi Lee,[‡] Chih-Li Lin,[§] Tzu-Huei Tu,[‡] Ling Hsuan Chen,[‡] Yi Jing Chen,[‡] and Hsiu-Chen Huang*[,‡]

[†]National Research Institute of Chinese Medicine, Taipei 11221, Taiwan

[‡]Department of Applied Science, National Hsinchu University of Education, Hsinchu 30014, Taiwan

[§]Institute of Medicine, Chung Shan Medical University, Taichung, Taiwan

**ABSTRACT:** Breast cancer is the most universal cancer in women, but the medications for breast cancer usually cause serious side effects and offer no effective treatment for triple-negative breast cancer. Here, we investigated the growth inhibitory effects of gallic acid (GA), (−)-epigallocatechin gallate (EGCG), or 1,2,3,4,6-penta-*O*-galloyl-*β*-D-glucose (5GG) combined with quercetin (Que) on breast cancer cells. In this study, we tested the combined effects of these compounds on estrogen receptor (ER)/human epidermal growth factor 2 (Her2)-negative (MDA-MB-231), ER-positive/Her2-negative (BT483), and ER-negative/Her2-positive (AU565) breast cancer cells. After treatment of each cell line with these compounds, we found that Que combined with 5GG induced S-phase arrest and apoptosis in MDA-BM-231 cells through downregulation of S-phase kinase protein 2 expression, but induced G2/M-phase arrest and apoptosis in AU565 cells through downregulation of Her2 expression. Additionally, Que combined with 5GG was more effective in inhibiting MDA-MB-231 cell growth than Que combined with EGCG (5GG analogue) or GA. The combination of 5GG and Que can offer great potential for the chemoprevention of ER-negative breast cancer.

**KEYWORDS:** *AU565, 5GG, MDA-MB231, Que, synergistic effect*

## 1. INTRODUCTION

Breast cancer is the most common cancer in women, and it is the second leading cause of cancer death among females. Traditional prognostic and clinicopathological factors in breast cancer include tumor size and grade, lymph node status, and the expression of receptors to estrogen (ER), progesterone, and human epidermal growth factor receptor 2 (Her2).[1] These markers of breast cancers can be employed for cancer detection and as targets for therapies. Targeted therapy with tamoxifen and trastuzumab is available for ER-positive and Her2-overexpressing breast tumors, respectively. However, no specific therapy has been identified in those tumors that are both ER- and Her2-negative. Recent clinical studies showed that a higher expression of S-phase kinase protein 2 (SKP2) occurs in ER-/Her2-negative and ER-positive/Her2-negative breast cancer cells, especially in triple-negative breast cancer cells.[2] Unfortunately, specific drugs that target SKP2 are unavailable at present. Therefore, it is important to develop SKP2 inhibitors as chemopreventive agents. In addition, the medications for breast cancer usually cause serious side effects and offer no effective treatment for triple-negative breast cancer. Flavonoids have been reported to suppress breast cancer cell growth without any significant side effects.[3]

3,3′,4′,5,7-Pentahydroxyflavone (quercetin, Que), a ubiquitous dietary flavonoid, has antioxidant, antitumor, and anti-inflammatory effects. Among flavonoids, Que was considered an excellent free radical-scavenging antioxidant. Apart from antioxidant activity, Que also exerted antiproliferative and proapoptotic effects in multiple cancer cell types, including liver,[4] breast,[5] prostate,[6] leukemia,[7] gastric,[8] colon,[9] and lung[10] cancer and animal models. Moreover, it killed tumor cells selectively without damaging normal cells.[11] Que could also increase the effectiveness of chemotherapeutic agents and other flavonoids. For instance, several recent reports showed that Que in combination with doxorubicin, tamoxifen, resveratrol, and catechin, respectively, was more potent than either agent alone in suppressing breast cancer growth.[5,12,13] Several clinical trials have reported using Que in patients with inflammatory-prone diseases, but no studies have yet been done using Que to treat patients with cancer.[14]

1,2,3,4,6-Penta-*O*-galloyl-*β*-D-glucose (pentagalloylglucose, 5GG) is structurally similar to (−)-epigallocatechin gallate (EGCG) in that it contains gallate moieties and an important component in traditional Chinese crude drugs. 5GG has recently been reported to induce cell cycle arrest and apoptosis in leukemia,[15] breast,[16] and prostate[17] cancer cells. Kim et al. reported that 5GG in combination with cisplatin synergistically induced apoptosis in renal cancer cells.[18] Although the anticancer activities of 5GG have attracted scientific attention, the detailed mechanisms of 5GG in breast cancer prevention have not been fully deciphered.

Many studies have shown that the combined use of several drugs with different mechanisms of action can exhibit additive

Received: December 10, 2012
Revised: June 3, 2013
Accepted: June 4, 2013
Published: June 4, 2013





dx.doi.org/10.1021/jf305253m | J. Agric. Food Chem. 2013, 61, 6430−6445

or synergistic preventive effects.[19,20] Therefore, multiple drugs may be more effective in the treatment of breast cancer than a single-drug treatment. In accordance with this concept, the ideal regimen would contain at least two active drugs. Previous studies showed that Que was a natural product and could inhibit cancer cell growth, and the anticancer mechanisms of Que were different from those of galloyl moiety structural analogues (gallic acid, EGCG, and 5GG) (Figure 1).[21]

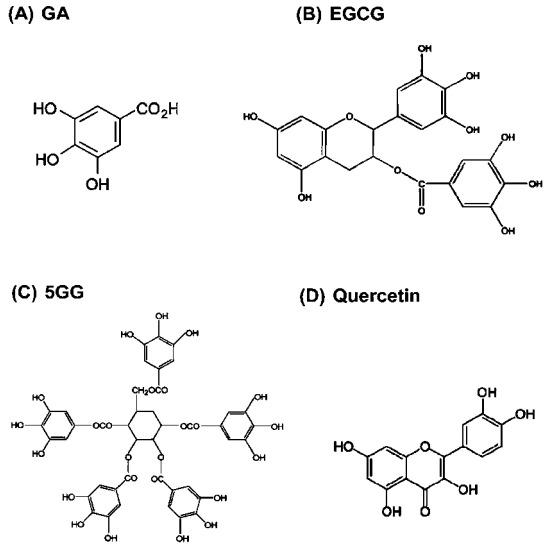


**Figure 1.** Chemical structure of (A) gallic acid (GA), (B) (−)-epigallocatechin gallate (EGCG), (C) 1,2,3,4,6-penta-*O*-galloyl-*β*-D-glucose (pentagalloylglucose, 5GG), and (D) quercetin.

However, previous studies have not examined whether the combination of 5GG and Que exerts a synergistic effect against cancer cells. Therefore, this study aimed to examine the combined effects of co-treatment with Que plus gallic acid (GA, part of the EGCG and 5GG ester), EGCG, and 5GG, respectively, on ER/Her2-negative (MDA-MB231), ER-positive/Her2-negative (BT483), and ER-negative/Her2-positive (AU565) breast cancer cells.

## 2. MATERIALS AND METHODS

**2.1. Chemicals.** 5GG was isolated from the leaves of *Macaranga tanarins* (L.) Muell. *et* Arg. as described previously.[22] Que, GA, EGCG, LY294002, dimethyl sulfoxide (DMSO), *N*-acetyl-Leu-Leu-norLeu-al (LLnL), NU6102, and 3-(4,5-dimethylthiazol-2-yl)-2,5-diphenyl tetrazolium bromide (MTT) were purchased from Sigma Chemical Co. (St. Louis, MO, USA). Antibodies for SKP2, cullin 1, CKS1, p27, cyclin A, cyclin B, cyclin D1, cyclin E, cdk1, cdk2, cdk4, cdk7, *β*-actin, *α*-tubulin, NF-*κ*B, and lamin C were purchased from Santa Cruz Biotechnology, Inc. (Santa Cruz, CA, USA). Phosphorylation state-specific antibodies were purchased from Cell Signaling Technology (Beverly, MA, USA). *β*-Actin antibody was from Abcam Inc. (Cambridge, MA, USA). Anti-mouse and anti-rabbit antibodies conjugated to horseradish peroxidase were obtained from Santa Cruz Biotechnology, Inc.. All other reagents and chemicals were purchased from Sigma and were of analytical grade.

**2.2. Cell Culture.** The human breast cancer cell lines used in this study were MDA-MB-231, BT483, and AU565. These cells were cultured in Dulbecco's modified Eagle's medium (DMEM) supplemented with 10% fetal calf serum and 1% penicillin–streptomycin. The MDA-MB-231.eB cells (which are MDA-MB-231 cells stably expressing wt ErbB2, SKP2/Her2 overexpression) were kindly provided by Dr. Mien-Chie Hung (University of Texas, M. D. Anderson Cancer Center, Houston, TX, USA) and were cultured as previously described.[23] These cells were grown at 37 °C in a humidified atmosphere of 5% $CO_2$.

**2.3. Cell Viability Assay.** Cells were seeded at $2 \times 10^4$ cells/well in a 24-well plate for 24 h, treated with varying concentrations of Que, 5GG, EGCG, GA, LY294002, or NU6102, and incubated for the indicated times. The effect of Que, 5GG, EGCG, GA, LY294002, or NU6102 on cell viability was examined by MTT assay. In brief, 20 μL of 5 mg/mL MTT solution was added to each well, followed by incubation at 37 °C for 3 h. Then, 200 μL of DMSO was added to each well. Finally, the absorbance of the oxidized MTT solution was detected by ELISA reader, at a wavelength of 550 nm.

**2.4. Morphological Features of Breast Cancer Cells.** After incubation with various reagents, the cells were fixed with 4% formaldehyde. Morphological changes in cells were examined by light microscopic observation.

**2.5. Flow Cytometry.** First, $1 \times 10^6$ cells were cultured in 10 cm Petri dishes and incubated for the indicated times. Then cells were harvested by trypsinization, washed with ice-cold PBS, resuspended in 200 μL of PBS, and fixed in 800 μL of iced 100% ethanol at −20 °C. After overnight, the cell pellets were collected by centrifugation, resuspended in 1 mL of buffer (0.5% Triton X-100 in PBS and 0.5 μg/mL RNase), and incubated at 37 °C for 30 min. Then, 1 mL of propidium iodide (PI) solution (50 μg/mL) was added and allowed to stand on ice for 30 min. Fluorescence emitted from the PI-DNA complex was quantified, after excitation of the fluorescent dye by FACScan cytometry.

**2.6. Analysis of Nuclear Morphology.** MDA-MB-231 and AU565 cells were plated on coverslips placed in six-well plates. After treatment with 5GG plus various concentrations of Que for 48 h, the cells were fixed with 4% formaldehyde for 20 min and incubated in 4 mg/mL Hoechst 33258 for 30 min. Coverslips were washed and mounted in Vectashield (Vector Laboratories, Burlingame, CA, USA), and the morphology of nuclear chromatin was viewed under a Leica TCS SP2 confocal laser-scanning microscope (Leica Microsystems, Heidelberg, Germany).

**2.7. DNA Fragmentation.** The cells were incubated with reagents of various dosage concentrations. Cells were washed with PBS and then lysed with lysis buffer containing 5 mM Tris buffer (pH 7.5), 0.5% Triton X-100, 0.5 mg/mL protease K, and 10 mM EDTA at 55 °C for 2 h and then treated with 0.5 μg/mL RNase A for another 1 h at 37 °C. The DNA was extracted by phenol/chloroform/isoamyl alcohol and then resuspended in TE buffer and analyzed by 2% agarose gel electrophoresis.

**2.8. Immunoblotting (Western Blotting).** The cells were treated with various agents, as indicated in the figure legends. After treatment, cells were placed on ice, washed with cold PBS, and lysed in gold lysis buffer. Protein content was quantitated by a Bio-Rad protein assay kit (Bio-Rad Laboratories). Each protein sample (50 μg) was separated on 10% sodium dodecyl sulfate-polyacrylamide gel (SDS-PAGE) and electrotransferred to a polyvinylidene difluoride (PVDF) membrane (Immobilon$^P$, Millipore, Bedford, MA, USA). Nonspecific binding on the PVDF membranes was minimized with a blocking buffer containing 1% bovine serum albumin (v/v) in PBS at room temperature for 1 h. Then the membranes were incubated with a different primary antibody, followed by secondary anti-rabbit/goat/mouse IgG conjugated with horseradish peroxidase. The immunoreactive bands were visualized with enhanced chemiluminescent reagents (ECL, Amersham). The intensity of the bands was quantified using Bio-Rad PDQuest Image software.

**2.9. Reverse Transcription Polymerase Chain Reaction (RT-PCR).** Total RNA was isolated from cultured cells using a REzol reagent. Reverse transcription was performed with the RNA templates, using Moloney murine leukemia virus (MMLV) reverse transcriptase and oligo (dT) 18 primer. The amplification of the cDNA was performed by polymerase chain reaction (PCR) in a final volume of 50 μL containing 2 μL of reverse transcription product, all four deoxynucleotide triphosphates (each at 200 μM), 1× reaction buffer, a 1 μM concentration of each primer, and 50 units/mL Pro Taq DNA polymerase. The amplification cycles were 95 °C for 30 s, 55 °C for 1


dx.doi.org/10.1021/jf305253m | J. Agric. Food Chem. 2013, 61, 6430−6445

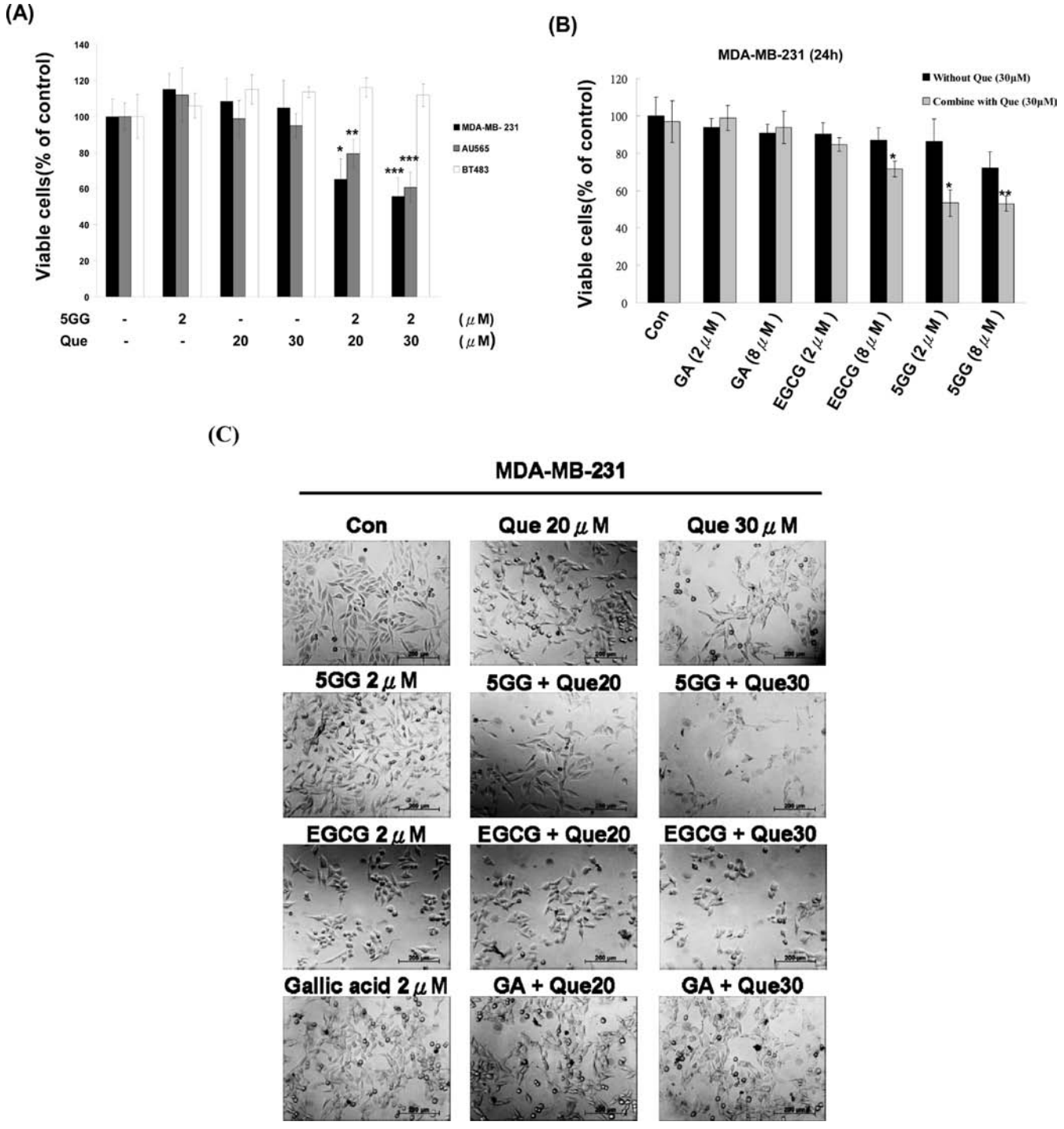


**Figure 2.** Effect of Que and galloyl moiety structural analogues (GA, EGCG, and 5GG) on the viability of breast cancer cells. (A, B) Cells were cultured in DMEM supplemented with 10% fetal calf serum for 24 h. After culturing for 24 h, cells were treated with DMSO, Que, GA, EGCG, 5GG, and Que plus GA, EGCG, and 5GG, respectively, for 24 h. Cell growth inhibition was determined by MTT assay. The number of viable cells after treatment is expressed as a percentage of the vehicle-only control. Data are the mean ± SE of three independent experiments. Co-treatments with Que plus GA, EGCG, and 5GG, respectively, were more effective than treatment with either agent alone: *, $p < 0.05$; **, $p < 0.01$; ***, $p < 0.001$ by ANOVA followed by Dunnett's multiple comparison test. (C) Morphological changes of cells were induced by Que plus GA, EGCG, and 5GG, respectively, for 24 h. Cells were treated with DMSO, Que, GA, EGCG, 5GG, and Que plus GA, EGCG, and 5GG, respectively, at the indicated concentrations for 24 h. Morphological changes in cells were examined by light microscopic observation. The bar in the images represents 200 μm in length.

min, and 72 °C for 1 min. The PCR products were separated by electrophoresis on a 1.5% agarose gel after 30 cycles and visualized by ethidium bromide staining. The sense and antisense primer sequences were CDK2: 5′-CGCTTCATGGAGAACTTC-3′ and 5′-ATGGCA-GAAAGCTAGGCC-3′; CDK4: 5′-CCCGCTTTCGTAGTTTT-CAT-3′ and 5′-TTATTTGAGCTTTGGTTCTG-3′; SKP2: 5′-ACAGTGAGAACATCCCC -CAG-3′ and 5′-GGTCCATAAAT-GATCGTGG-G-3′; glyceraldehyde-3-phosphate dehydrogenase (GAPDH): 5′-TGAAGGTCGGTGTGAACGGATTTGGC-3′ and 5′-CATGTAGGCCATGAGGTC CACCAC-3′.


dx.doi.org/10.1021/jf305253m | J. Agric. Food Chem. 2013, 61, 6430−6445

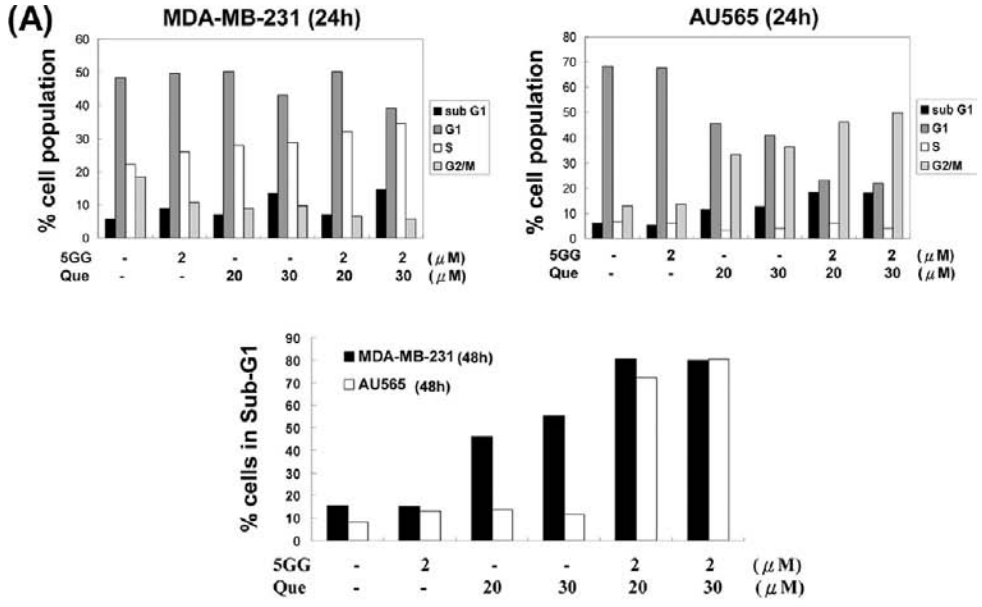


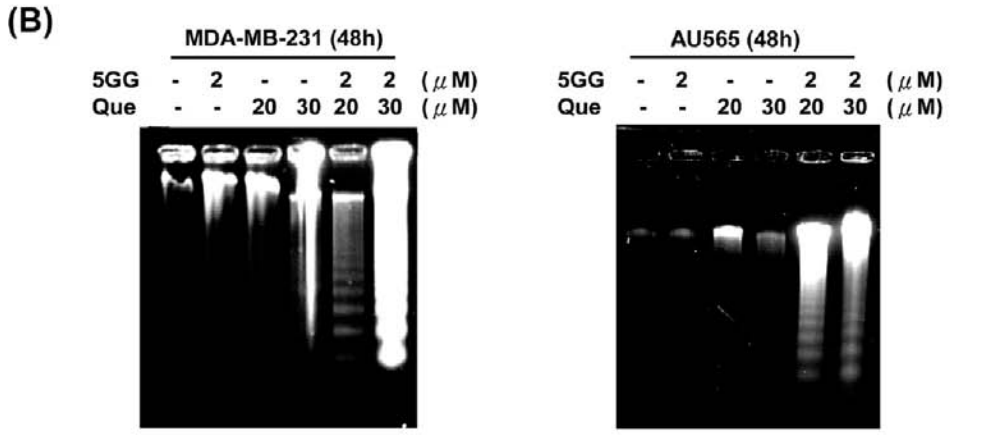


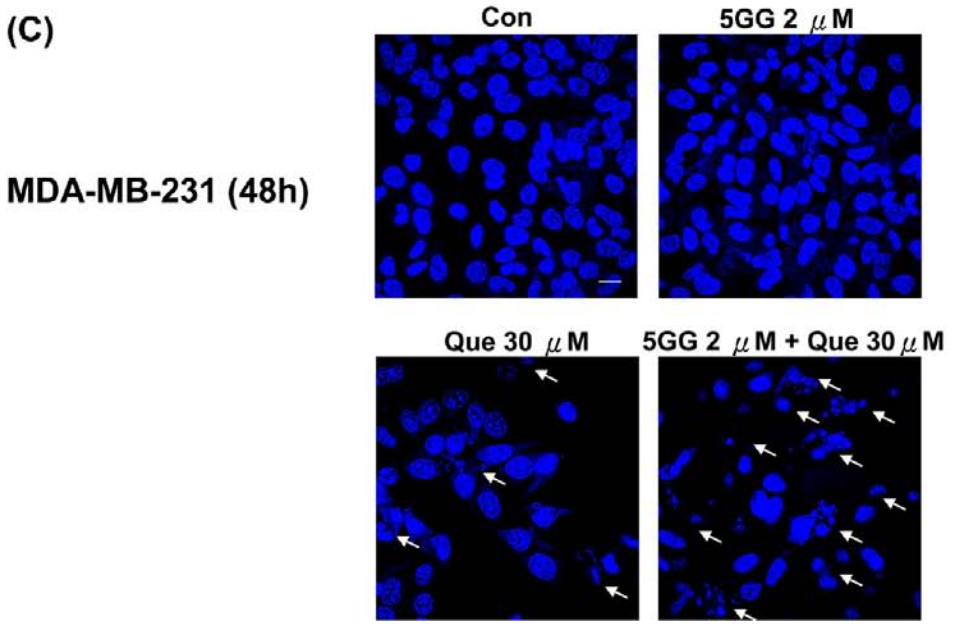


**Figure 3.** continued


dx.doi.org/10.1021/jf305253m | J. Agric. Food Chem. 2013, 61, 6430−6445

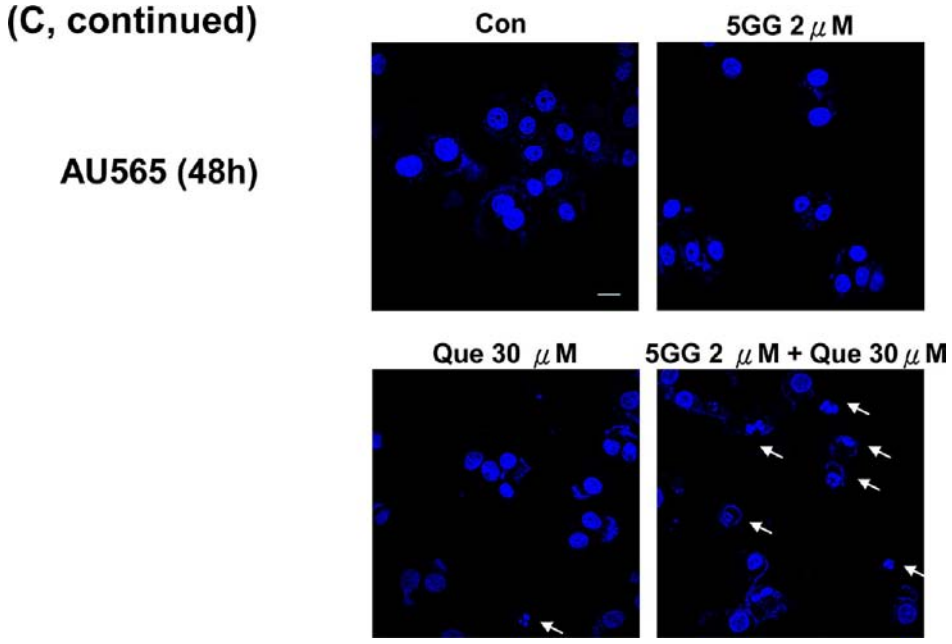


**Figure 3.** Changes in cell cycle phase distribution following co-treatment with 5GG plus Que. (A) MDA-MB-231 and AU565 cells were cultured in DMEM supplemented with 10% fetal calf serum for 24 h. After culturing for 24 h, cells were treated with DMSO, Que, 5GG, and Que plus 5GG, respectively, for 24 and 48 h. Cells were then harvested and stained with propidium iodide, and cell cycle distribution was analyzed by flow cytometry. (B) Effect of Que plus 5GG on the morphology of nuclear chromatin in both breast cancer cells. Cells were co-treated with DMSO, Que, 5GG, and Que plus 5GG, respectively, for 48 h and stained with Hoechst 33258, as described in the Materials and Methods section. The morphological changes in nuclear chromatin were then viewed under a fluorescence microscope. The bar in the images represents 10 $\mu$M in length. (C) The cytotoxic effect in both breast cancer cells co-treated with Que plus 5GG is examined using the DNA fragmentation assay as described in the Materials and Methods.

**2.10. Preparation of Nuclear and Cytosolic Extracts.** The cells were suspended in hypotonic buffer—HEPES (pH 7.6) 10 mM, EDTA 0.1 mM, dithiothreitol (DTT) 1 mM, and PMSF 0.5 mM—for 10 min on ice and vortexed for 10 s. Nuclei were pelleted down by centrifugation at 12000*g* for 20 s. The supernatants (cytosolic protein) were collected, and the pellet was suspended in hypertonic buffer—EDTA 1 mM, DTT 1 mM, PMSF 0.5 mM, 25% glycerol, 0.4 M NaCl—for 30 min on ice. The nuclear proteins were collected by centrifugation at 12000*g* for 20 min. Nucleus and cytosolic extracts were prepared and then subjected to immunoblot analysis.

**2.11. Immunofluorescence Assay.** MDA-MB-231 cells were plated on coverslips placed in six-well plates. Cells were fixed with 4% formaldehyde for 20 min, rinsed with PBS, and then blocked with a blocking buffer containing 1% bovine serum albumin (v/v) in PBS for 1 h. Incubations were performed with primary antibodies diluted in blocking buffer at 4 °C overnight, after which coverslips were washed with PBS and incubated for 30 min with the fluorescein isothiocyanate-conjugated secondary antibodies diluted in PBS. Then, cells were incubated in 4 mg/mL Hoechst 33258 for 30 min. Coverslips were washed and mounted in Vectashield and viewed under a Leica TCS SP2 confocal laser-scanning microscope.

**2.12. RNAi Suppression of SKP2.** Logarithmically growing MDA-MB-231 cells were seeded at a density of $1 \times 10^5$ cells/well in six-well plates in serum-containing medium. The SKP2 p45 siRNA gene silencer (human) dsRNA was obtained from Santa Cruz Biotechnology. MDA-MB-231 cells were transfected with dsRNAs using siRNA transfection reagent (Santa Cruz) and incubated for 6 h. Then, the cells were analyzed by immunoblot for SKP2, cullin 1, CDK2, CDK4, cyclin B, cyclin D1, sirt1, survivin, acetyl-P53(Lys382), caspase 3, and $\beta$-actin expression. Cell viability was assessed using the MTT assay. Cell cycle progression was assessed using flow cytometry.

**2.13. Soft Agar Colony Formation Assay.** Briefly, single-cell suspensions of MDA-MB-231 cells were treated with DMSO alone (con), Que alone, and 5GG alone or co-treated with Que and 5GG and then mixed with agarose in a final concentration of 0.35%. Aliquots of 2 mL containing $1 \times 10^4$ cells and 10% FCS were plated in triplicate in 6 cm culture dishes over a base layer of 0.7% agarose and allowed to gel. Colonies of >60 $\mu$m were counted after the indicated time of incubation.

**2.14. Statistical Analysis.** All values were expressed as mean ± SE. Each value is the mean of at least three separate experiments in each group. Student's *t*-test was used for statistical comparison. * indicates that the values are significantly different from the control (*, $p < 0.05$; **, $p < 0.01$; ***, $p < 0.001$). Multiple group comparisons were performed using ANOVA followed by Dunnett's multiple comparison test to assess statistical significance (*, $p < 0.05$; **, $p < 0.01$; ***, $p < 0.001$). The combination index (CI) was calculated to asses synergistic effect (CI < 1) or additive effect (CI = 1). CI was defined as follows: CI = (D)1/(D*x*)1 + (D)2/(D*x*)2 + (D)1(D)2/(D*x*)1(D*x*)2, where (D*x*)1 and (D*x*)2 are the concentrations of drug 1 and drug 2, which alone produce *x*% effect; (D)1 and (D)2 are the concentrations of drug 1 combined with drug 2 to obtain the same response as drug 1 alone or drug 2 alone.

## 3. RESULTS

**3.1. Growth Inhibitory Effects of 5GG Combined with Que in ER-Positive and ER-Negative Breast Cancer Cells.** The combined effects of 5GG and Que were evaluated using MTT assay and combination index in one ER-positive (BT483) and two ER-negative (MDA-MB-231 and AU565) breast cancer cells. After 24 h of incubation with 2 $\mu$M 5GG alone, the number of viable cells in MDA-MB-231 was 100% of that in the control, whereas the number after incubation with 20 and 30 $\mu$M Que alone was 98.4% and 85.3%, respectively. Co-treatment with 5GG plus 20 and 30 $\mu$M Que reduced the number of viable cells to 57.5% and 40.9%, respectively (Figure 2A). The calculated CI values for 5GG plus 20 and 30 $\mu$M Que were consistently <1, indicating synergism. Similar results were also observed in AU565 breast cancer cells. Co-treatment with 5GG plus Que for 24 h synergistically reduced cell growth in

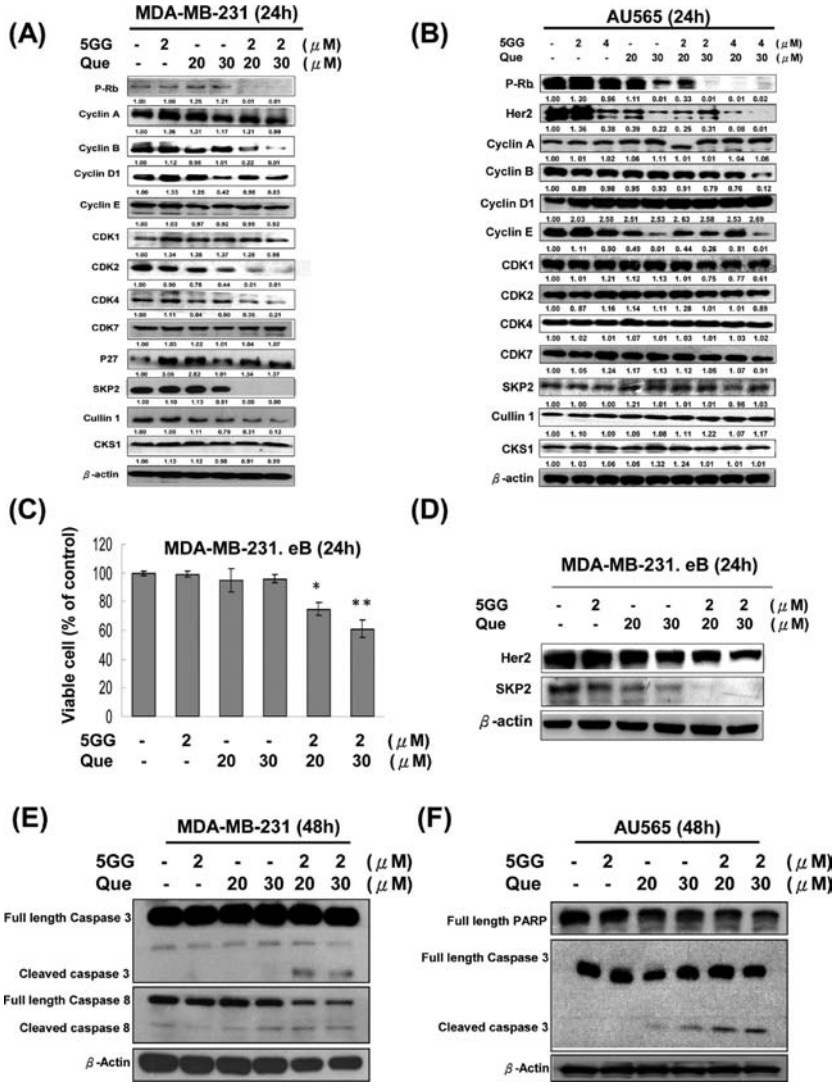


**Figure 4.** Effects of co-treatment with 5GG plus Que on cell cycle regulatory protein and apoptosis regulatory protein expression in MDA-MB-231 and AU565 cells. MDA-MB-231 and AU565 cells were cultured in DMEM supplemented with 10% fetal calf serum for 24 h. After culturing for 24 h, both cell lines were treated with DMSO, Que, 5GG, and Que plus 5GG, respectively, for 24 and 48 h. Expressions of cell cycle regulatory protein (A, B) and apoptosis regulatory proteins (E, F) in both cells co-treated with 5GG plus Que were determined by Western blot analysis. $\beta$-Actin was used as an internal control to ensure equivalent protein loading. The values below the figures represent changes in protein level of the bands normalized to DMSO-treated control. (C) MDA-MB-231.eB cells were treated with DMSO, Que, 5GG, and Que plus 5GG, respectively, for 24 h. Cell growth inhibition was determined by the MTT assay. The number of viable cells after treatment is expressed as a percentage of the vehicle-only control. Data are the mean ± SE of three independent experiments. Co-treatment was more effective than treatment with either agent alone: *, $p < 0.05$; **, $p < 0.01$; ***, $p < 0.001$ by ANOVA followed by Dunnett's multiple comparison test. (D) Both SKP2 and Her2 expressions of MDA-MB-231eb cells co-treated with 5GG plus Que were determined by Western blot analysis.

AU565 and MDA-MB-231 cells, but not in BT483 cells, revealing that 5GG when combined with Que had a synergistic effect on the inhibition of ER-negative breast cancer cell growth. Thus, AU565 and MDA-MB-231 cell lines were selected for further analysis.

**3.2. Morphological Changes and Growth Inhibitory Effects of GA, EGCG, or 5GG Combined with Que on MDA-MB-231 Cells.** 5GG contains five gallate moieties linked with a glucose core by an ester bond. 5GG is structurally similar to EGCG, which contains one gallate moiety linked with epigallocatechin by an ester bond. To test whether the presence of a gallate moiety could enhance the growth inhibitory ability of Que, MDA-MB-231 cells were treated independently with 2 or 8 $\mu$M GA, EGCG, or 5GG alone or combined with 30 $\mu$M Que, and cell growth was evaluated by MTT assay. As shown in Figure 2B, 8 $\mu$M GA, 8 $\mu$M EGCG, 8 $\mu$M 5GG, and 30 $\mu$M Que independently decreased MDA-MB-231 cell viability by approximately 8.8%, 9.1%, 33.2%, and 13.5%, respectively. However, Que plus GA, EGCG, and 5GG, respectively, decreased cell viability by approximately 5.2%, 38.6%, and 59.4%, respectively. The morphological changes in MDA-MB-231 cells co-treated with different concentrations of Que plus GA, EGCG, and 5GG, respectively, for 24 h are illustrated in Figure 2C. The control cells were tightly attached not only to the culture plate but also to each other and formed a confluent layer of flat cells. By contrast, the morphology of MDA-MB-231 cells changed dramatically after co-treatment with Que plus EGCG or Que plus 5GG, but not after treatment with each agent alone or co-treatment with Que plus GA. These findings indicate that Que combined with compounds containing the


dx.doi.org/10.1021/jf305253m | J. Agric. Food Chem. 2013, 61, 6430−6445

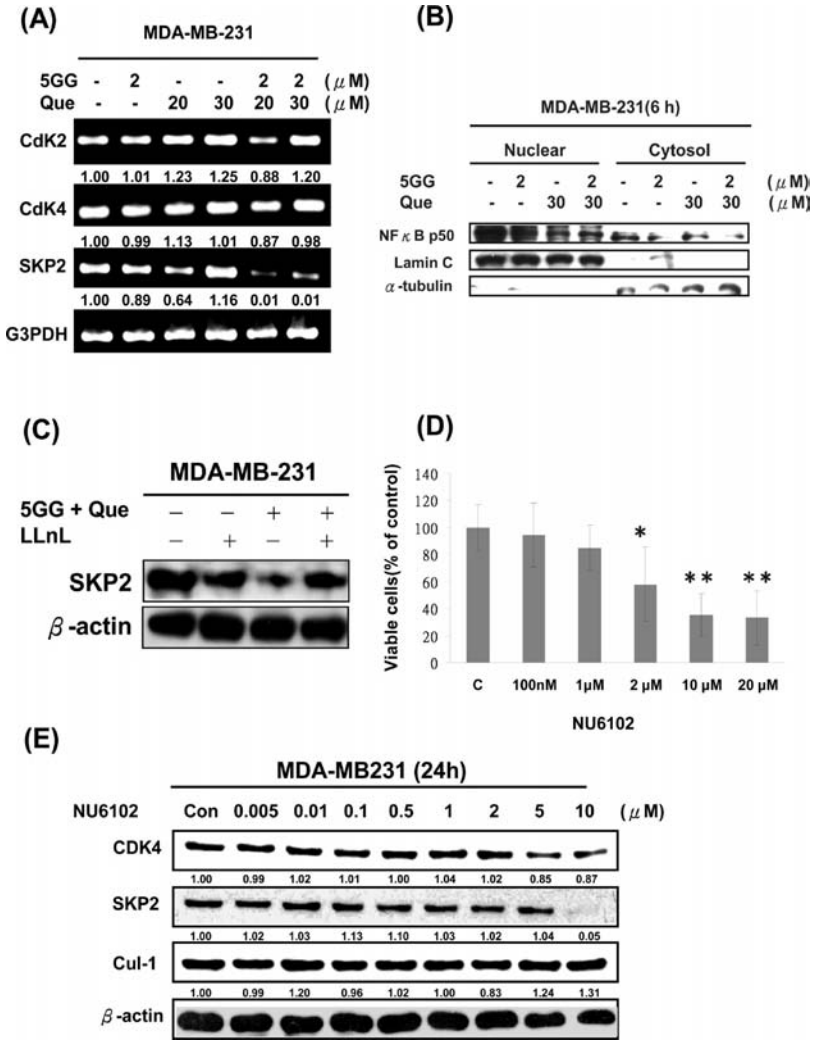


**Figure 5.** Mechanism of downregulation of SKP2 by co-treatment with Que plus 5GG in MDA-MB-231 cells. (A) MDA-MB-231 cells were treated with DMSO, Que, 5GG, and Que plus 5GG, respectively, for 24 h. Total RNA was isolated, and the mRNA expression was analyzed by reverse transcription-polymerase chain reaction (RT-PCR), as described in the experimental procedures. The values below the figures represent changes in mRNA level of the bands normalized to the control. (B) Effects of co-treatment with 5GG plus Que on NF-κB (p50) activation in MDA-MB-231. Cells were treated with DMSO, Que, 5GG, and Que plus 5GG, respectively, for 6 h. After the isolation of nuclear and cytoplasm extracts, nucleus translocation of the NF-κB p50 subunit was measured by Western blot analysis. Lamin B and β-tubulin were used as the nuclear and cytosol fraction markers, respectively. (C) Effect of LLnL pretreatment on SKP2 protein in MDA-MB-231 cells exposed to 5GG combined with Que. Total cell lysates of MDA-MB-231 cells treated with 5GG combined with Que for 24 h in the presence or absence of a half-hour pretreatment of 5 μM LLnL were harvested and then analyzed by Western blot analysis with SKP2 and β-actin antibodies. (D) MDA-MB-231 cells were treated with different concentrations of NU6102. Cell growth inhibition was determined by MTT assay. The number of viable cells after treatment is expressed as a percentage of the vehicle-only control. Data are the mean ± SE. Each value is the mean of at least three separate experiments in each group. Student's *t*-test was used for statistical comparison. * indicates that the values are significantly different from the control (*, $p < 0.05$; **, $p < 0.01$; ***, $p < 0.001$). (E) MDA-MB-231 cells were treated with DMSO alone (Con) and different concentrations of NU6102 for 24 h. Total cell lysates were prepared, and Western blot analysis was performed. The experiment was performed three times for each antibody, with each yielding similar results. β-Actin was used as an internal control to ensure equivalent protein loading. The values below the figures represent changes in protein level of the bands normalized to the DMSO-treated control.

gallate moiety had a synergistic or additive effect on the inhibition of MDA-MB-231 cell growth.

**3.3. 5GG Combined with Que Synergistically Induced Cell Cycle Arrest and Apoptosis in MDA-MB-231 and AU565 Cells.** In order to study the mechanisms underlying the synergy between 5GG plus Que in growth inhibition of breast cancer cells, cell cycle analyses were performed on both AU565 and MDA-MB-231 cells after 24 and 48 h of drug exposure, using flow cytometric analysis of cellular DNA content. Treatment of MDA-MB 231 cells with 20 and 30 μM Que alone for 48 h significantly increased the percentage of cells in the sub-G1 phase (45.97−55.3%). Co-treatment of MDA-MB 231 cells with 2 μM 5GG plus 20 and 30 μM Que resulted in a significantly higher percentage of cells in the S phase (32.03−34.49%) at 24 h and in the sub-G1 phase (80.43−80.03%) at 48 h, compared with treatment using either of the two agents alone (Figure 3A). In AU565 cells, treatment with 20 and 30 μM Que alone for 24 h significantly increased the percentage of cells in the G2/M phase (33.1−36.3%). Co-treatment led to a much more extensive G2/M-phase accumulation (46.21−49.81%) at 24 h and sub-G1-phase accumulation (72.11−80.61%) at 48 h, compared with treatment by either agent

alone at the same concentrations. These results demonstrate that 5GG plus Que acted synergistically to induce cell cycle arrest and apoptosis in both breast cancer cells.

We next assessed the effect of 5GG combined with Que on the induction of apoptosis in AU565 and MDA-MB-231 cells by the DNA fragmentation assay and Hochest assay. Treatment of MDA-MB-231 cells with 2 $\mu$M 5GG or 20 $\mu$M Que alone for 48 h did not induce DNA fragmentation. However, co-treatment with 2 $\mu$M 5GG plus 20 $\mu$M Que induced dose-dependent DNA fragmentation (Figure 3B). The induction of apoptosis by co-treatment with 5GG plus Que in MDA-MB-231 cells was further confirmed in fluorescence photomicrographs of cells stained with Hoechst 33258 after co-treatment with 2 $\mu$M 5GG plus 30 $\mu$M Que for 48 h. The control cells showed round and homogeneous nuclei, whereas cells co-treated with 2 $\mu$M 5GG plus 30 $\mu$M Que showed condensed and fragmented nuclei (Figure 3C). Similar results were also observed in AU565 breast cancer cells (Figure 3B and C).

**3.4. Combined Effect of 5GG Plus Que in Modulating Expression Levels of Cell Cycle and Apoptosis Regulatory Proteins in MDA-MB-231 and AU565 Cells.** The mechanisms underlying the induction of cell cycle arrest and apoptosis in MDA-MB 231 and AU565 cells exposed to 5GG and Que in various concentrations alone or in combination were examined. Figure 4A shows that 5GG and Que alone, or in combination, did not decrease cyclin A, cyclin D1, cyclin E, CDK1, CDK7, or CKS1 protein expression in MDA-MB-231 cells. However, co-treatment with 5GG plus Que for 24 h could synergistically decrease P-RB, cyclin B, CDK2, CDK4, SKP2, and cullin 1 in MDA-MB-231 cells. These results show the synergistic action of 5GG plus Que on S-phase cell cycle arrest in MDA-MB-231 cells through downregulating P-RB, cyclin B, CDK2, CDK4, SKP2, and cullin 1. Our previous study has demonstrated high expression of SKP2 in MDA-MB-231 cells. Unlike MDA-MB-231 cells (SKP2-overexpressing cell line), AU565 cells (Her2-overexpressing cell line) co-treated with 5GG plus Que synergistically decreased Her2, P-RB, cyclin B, and CDK1 expression, but not SKP2 expression (Figure 4B). Studies have shown a strong correlation of SKP2 and Her2 with breast cancer in many cases. To study the combined effect of 5GG plus Que on cell proliferation in MDA-MB-231.eB breast cancer cell lines (SKP2/Her2-overexpressing cell line), MDA-MB-231.eB cells were treated with various concentrations of 5GG and Que for 24 h. The combined treatment with 5GG and Que was synergistically effective in repressing cell proliferation in MDA-MB-231.eB cells through downregulation of SKP2 and Her2 protein (Figure 4C and D). The obtained results suggest that co-treatment with 5GG plus Que proved exceedingly effective and provided a basis for the development of potent agents that can pharmacologically target both SKP2 and Her2 in breast cancer.

Flow cytometry and DNA fragmentation data show that co-treatment with 5GG plus Que synergistically triggered apoptosis in MDA-MB-231 and AU565 cells. In view of this, Western blot analysis was employed to detect the protein expression levels of PARP, cleaved caspase 3, and caspase 8 for various doses of 5GG plus Que in MDA-MB-231 and AU565 cells (Figure 4E and F). The protein expression levels of cleaved caspase 3 in MDA-MB-231 and AU565 cells synergistically increased after co-treatment with 5GG plus Que for 48 h. Taken together, these results indicate that treatment using 5GG combined with Que can synergistically induce apoptosis in MDA-MB-231 and AU565 cells through caspase-3-dependent pathways.

**3.5. Effects of 5GG Combined with Que on mRNA Level of SKP2 in MDA-MB-231 Cells.** Previous results showed that co-treatment with 5GG plus Que for 24 h induced S-phase arrest in MDA-BM-231 cells. CDK2, CDK4, and SKP2 play important roles in the transition of G1 to S phase. To address the mechanism of how co-treatment with 5GG plus Que decreased the protein level of SKP2, CDK2, and CDK4, we first examined the mRNA level of SKP2, CDK2, and CDK4. A striking decrease in SKP2 mRNA was found in MDA-MB-231 cells after co-treatment with 5GG (2 $\mu$M) plus Que (20 and 30 $\mu$M) (Figure 5A), suggesting that the downregulation of SKP2 mRNA was, at least in part, attributable to the decrease in SKP2 protein expression. However, no significant change in CDK2 and CDK4 mRNA levels was observed in co-treated cells. These results indicate that co-treatment with 5GG plus Que induced a decrease in CDK2 and CDK4 protein levels, which involved a post-transcriptional mechanism in MDA-MB-231 cells. Previous reports have demonstrated that the SKP2 promoter has NF-kB transcription-factor-binding motifs.[24,25] To confirm the involvement of NF-kB in the regulation of SKP2 expression, we performed an NF-kB translocation assay in cells co-treated with 5GG plus Que. Nucleus and cytosolic extracts were prepared and subjected to Western blot analysis. Our data in Figure 5B demonstrated that the amount of NF-kB (p50) nuclear proteins was diminished by co-treatment with 5GG plus Que in comparison with the control after 6 h.

On the other hand, it is known that in the S phase SKP2 is downregulated by APC/$C^{Cdh1}$, an E3 ligase that polyubiquitynates SKP2.[26] To investigate whether the ubiquitin−proteasome system is engaged in the regulation of SKP2 protein by co-treatment with 5GG plus Que, MDA-MB-231 cells were incubated with 5GG plus Que in the presence or absence of LLnL (5 $\mu$ M), a proteasome inhibitor. Results show that the inhibitory effects of 5GG combined with Que on the SKP2 protein level were abolished in the presence of LLnL, suggesting that a posttranslational mechanism also contributed to SKP2 depletion in MDA-MB-231 cells after co-treatment with 5GG plus Que (comparison of lane 3 with lane 4 in Figure 5C).

Recent studies have shown that SKP2 expression was reduced when CDK4 expression was inhibited by CDK4-specific siRNA.[27] Furthermore, knockdown of SKP2 using SKP2-specific siRNAs could decrease CDK2 expression, but not CDK4 expression.[28] This study investigated whether knockdown of SKP2 can be mimicked using NU6102, which was a potent inhibitor of CDK1 ($IC_{50}$ = 9.5 nM), CDK2 ($IC_{50}$ = 9.5 nM), and CDK4 ($IC_{50}$ = 1.6 $\mu$M). The effect of NU6102 on MDA-MB-231 cells was also investigated. As shown in Figure 5D, NU6102 was a more potent inhibitor of MDA-MB-231 cell growth, with $IC_{50}$ values of 1.8 $\mu$M. The effect of NU6102 on CDK4, SKP2, and cullin 1 expression was also investigated. Exposure to 10 $\mu$M NU6102 was required to detect reduced SKP2 protein levels (Figure 5E). The results suggest that SKP2 expression was reduced when the CDK activity was inhibited by NU6102. In our previous study, we found that 5GG combined with Que could decrease CDK2, CDK4, and SKP2 protein levels. Taken together, these findings suggest that the dependent inhibition of SKP2 protein expression was associated with reduced CDK activity in MDA-MB-231 cells after co-treatment with 5GG plus Que.

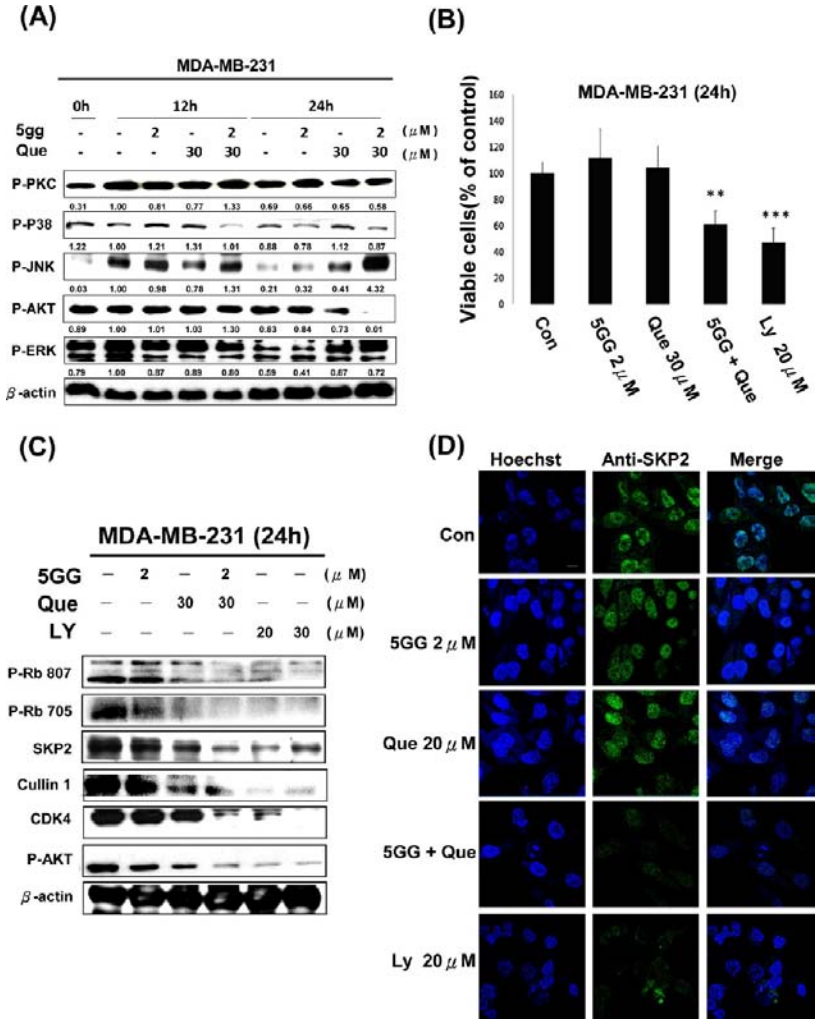


**Figure 6.** Combined effect of 5GG and Que on ERK, P38, JNK, PKC, and Akt phosphorylation in MDA-MB-231 cells. (A) Cells were treated with DMSO, Que, 5GG, and Que plus 5GG, respectively, for indicated times. Levels of phosphorylated ERK, P38, JNK, PKC, and Akt were analyzed by Western blot analysis with phopho-p44/42 ERK (Thr202/Tyr204), phospho-p38, phospho-JNK, phospho-PKC, and phospho-Akt (Ser-473) antibodies. The values below the figures represent changes in protein level of the bands normalized to 12 h-treated control. (B) Cells were treated with the PI3K inhibitor LY294002 (LY; 20 $\mu$M) for 24 h. Cell growth inhibition was determined by MTT assay. The number of viable cells after treatment is expressed as a percentage of the vehicle-only control. Data are the mean ± SE. Each value is the mean of at least three separate experiments in each group. Student's *t*-test was used for statistical comparison. * indicates that the values are significantly different from the control (*, $p < 0.05$; **, $p < 0.01$; ***, $p < 0.001$). (C) Cells were treated with DMSO, Que, 5GG, Que plus 5GG, and LY294002, respectively, for 24 h, and the expression levels of P-RB, SKP2, cullin 1, cyclin D1, and CDK4 were determined by Western blot analysis. (D) MDA-MB-231 cells grown on coverslips were treated with DMSO, Que, 5GG, and Que plus 5GG, respectively, for 24 h. Cells were fixed with 4% paraformaldehyde and stained with SKP2 antibody, followed by fluorescein isothiocyanate-conjugated secondary antibody (green) stained with Hoechst 33258 (blue). Analysis of subcellular distribution was performed by confocal microscopy. The bar in the images represents 10 $\mu$m in length.

**3.6. PI3k/Akt Pathway Involved in Growth Inhibition and SKP2 Downregulation Induced by Co-treatment with 5GG and Que in MDA-MB 231 Cells.** Akt, ERK, JNK, p38, and PKC have been shown to be involved in SKP2 regulation in various cell types.[29] Next, we explored the underlying signal transduction pathways of cell cycle arrest and apoptosis induced by 5GG combined with Que in MDA-MB 231 cells. We determined the effect of 5GG plus Que under different treatments during 12−24 h on the actions of PKC, ERK1/2, AKT, JNK, and P38. Cells were first co-treated with 2 $\mu$M 5GG plus 30 $\mu$M Que for different time periods, and the actions of PKC, ERK1/2, AKT, JNK, and P38 were measured by Western blot analysis using antiphosphorylated antibodies. As shown in Figure 6A, co-treatment with 5GG plus Que synergistically inhibited the phosphorylation of Akt at 24 h, but synergistically increased JNK and ERK1/2 phosphorylation at 24 h. However, co-treatment with 5GG plus Que for 24 h did not affect the phosphorylation of PKC and P38. In further studies, we examined whether growth inhibition and SKP2 downregulation induced by co-treatment with 5GG plus Que were mediated through the modulation of Akt phosphorylation. As shown in Figure 6B and C, treating the cells with the inhibitors of phosphatidylinositol 3-kinase (PI3K) (LY294002) significantly reduced cell growth and SKP2 protein expression. Akt activity can also influence SKP2 nuclear translocation. To determine whether the S-phase cell arrest induced by co-treatment with 5GG plus Que could be involved in the alteration of SKP2 subcellular localization, we performed immunofluorescence staining experiments to observe the localization of SKP2 in MDA-MB-231 cells. Immunofluor-

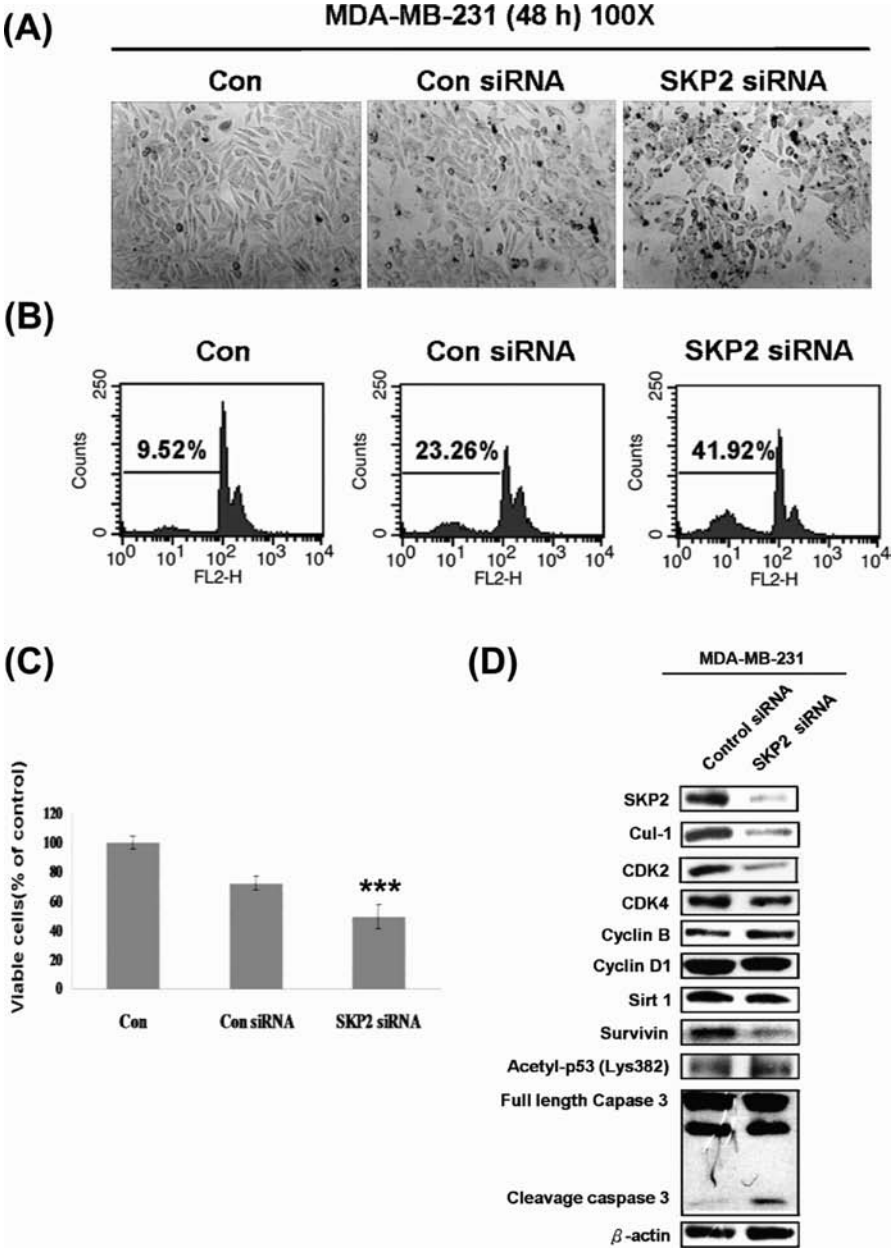


**Figure 7.** Morphology, cell cycle distribution, cell viability, and protein expression of MDA-MB-231 cells transfected with SKP2 siRNA. MDA-MB-231 cells were plated on 6 cm dishes and transfected with the control siRNA or SKP2 siRNA for 48 h. The morphological changes in cells were examined by light microscopic observation (100× original magnification) (A). Cells were then harvested and stained with propidium iodide, and cell cycle distribution was analyzed by flow cytometry (B). (C) MDA-MB-231 cells were plated on a 24-well plate and transfected with SKP2 siRNA or control siRNA for 48 h. Cells were then harvested, and cell viability was determined by MTT assay. The number of viable cells after treatment is expressed as a percentage of the vehicle-only control. Data are the mean ± SE. Each value is the mean of at least three separate experiments in each group. Student's *t*-test was used for statistical comparison. * indicates that the values are significantly different from the control siRNA (*, $p < 0.05$; **, $p < 0.01$; ***, $p < 0.001$). (D) Western blot analysis of SKP2, cell cycle-related, and apoptosis-related protein expression was performed 48 h after transfection. $\beta$-Actin was used as an internal control for equivalent protein loading.

escence showed that SKP2 protein was mainly expressed in nuclei of MDA-MB-231 cells, while co-treatment with 5GG plus Que synergistically decreased the nuclear localization of SKP2 (Figure 6D). Similar results were also observed in MDA-MB-231 cells treated with LY294002.

**3.7. Knockdown of SKP2 by RNA Interference Increased Caspase-Dependent Apoptosis in MDA-MB-231 Cells.** It is well known that SKP2 plays an important role in cell cycle progression. Recent studies have also shown that SKP2 inhibits cell apoptosis in breast cancer cells.[30] However, the mechanism of apoptosis induction by SKP2 is not well established in breast cancer. To explore the involvement of SKP2 in induction of apoptosis by co-treatment with 5GG plus Que, MDA-MB-231 cells were transfected with SKP2 siRNA for 48 h and SKP2 knockdown was examined by Western blot analysis. As shown in Figure 7A and C, both cell viability and morphology in SKP2 siRNA transfectants were affected compared with the control siRNA transfectants. Results of flow cytometry also demonstrated that the sub-G1 population was remarkably increased in SKP2 siRNA-transfected cells


dx.doi.org/10.1021/jf305253m | J. Agric. Food Chem. 2013, 61, 6430−6445

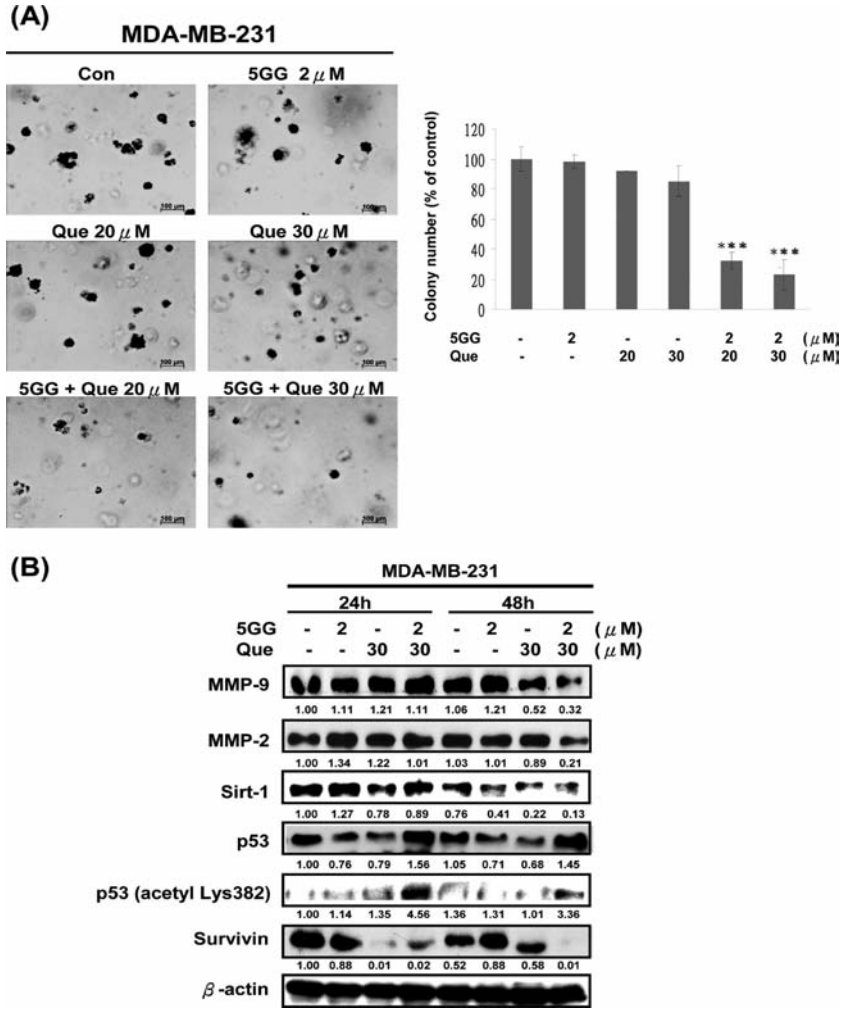


**Figure 8.** Combined effect of 5GG and Que on anchorage-independent growth of MDA-MB-231 breast cancer cells. (A) Effects of co-treatment with 5GG plus Que on colony formation of MDA-MB-231 cells were determined using the soft agar colony formation assay. Cells were treated with different concentrations of 5GG and Que in 0.35% agarose containing 10% FCS over 0.7% agarose containing 10% FCS. Cell colonies after 20-day incubation at 37 °C in 5% $CO_2$ were observed under light microscopy. The bar in the images represents 100 μm in length. Colonies of >60 μm were counted after 20 days of incubation. Data are the mean ± SE of three independent experiments. Co-treatment was more effective than treatment with either agent alone: *, $p < 0.05$; **, $p < 0.01$; ***, $p < 0.001$ by ANOVA followed by Dunnett's multiple comparison test. (B) Effect of co-treatment with 5GG plus Que on expression levels of MMP2, MMP9, Sirt1, p53, acetyl-p53, and survivin in MDA-MB-231 cells. The values below the figures represent changes in protein level of the bands normalized to 24 h-treated control.

compared with control siRNA (Figure 7B). RNA interference was carried out to investigate whether apoptosis-related protein levels would increase when MDA-MB-231 cells were transfected with SKP2 siRNA. SKP2 siRNA knocked down the protein levels of SKP2 in MDA-MB-231 cells compared with control siRNA transfectants. As expected, it also increased the protein levels of cleavage caspase 3 and acetyl-p53, but decreased the protein levels of cullin 1, CDK2, and survivin (Figure 7D).

**3.8. Combined Effect of 5GG and Que on Anchorage-Independent Growth of MDA-MB-231 Breast Cancer Cells.** Signoretti et al. reported that SKP2 is required for anchorage independence in breast epithelial cancer cells.[2] Yokoi et al. reported that knockdown of SKP2 by RNAi decreased anchorage-independent growth and metastasis in lung cancer cells.[31] To determine whether 5GG combined with Que may affect anchorage-independent proliferation potential, an important hallmark of the transformation, MDA-MB-231 cells co-treated with 5GG plus Que were plated in soft agar for 20 days. The soft agar can be used not only for separation of cancer cells but also for confirming whether the cells have cancerous characteristics. After 20 days in the cultures, co-treatment with 5GG plus Que synergistically reduced capacity for soft agar colony formation, with a smaller number of colonies formed and a reduced colony size (Figure 8A).

Many studies have indicated that SKP2 overexpression increases MMP2 and MMP9 protein expression and invasion of lung cancer cells.[32] Recent studies have also shown that SKP2 could decrease p53 activity and inhibit apoptosis.[33,34] After co-treatment with 5GG plus Que for 48 h, MMP2, MMP9, Sirt1, and survivin protein levels were synergistically reduced in MDA-MB-231 cells, but p53 and acetyl-p53 (Lys382) protein levels were synergistically increased in a time-dependent manner (Figure 8B). These findings imply that co-treatment with 5GG plus Que could modulate expressions of other SKP2 target proteins, including p53, MMP2, and MMP9.

**3.9. Combination of Tamoxifen and 5GG Synergistically Induces Apoptosis in MDA-MB-231 Cells through**

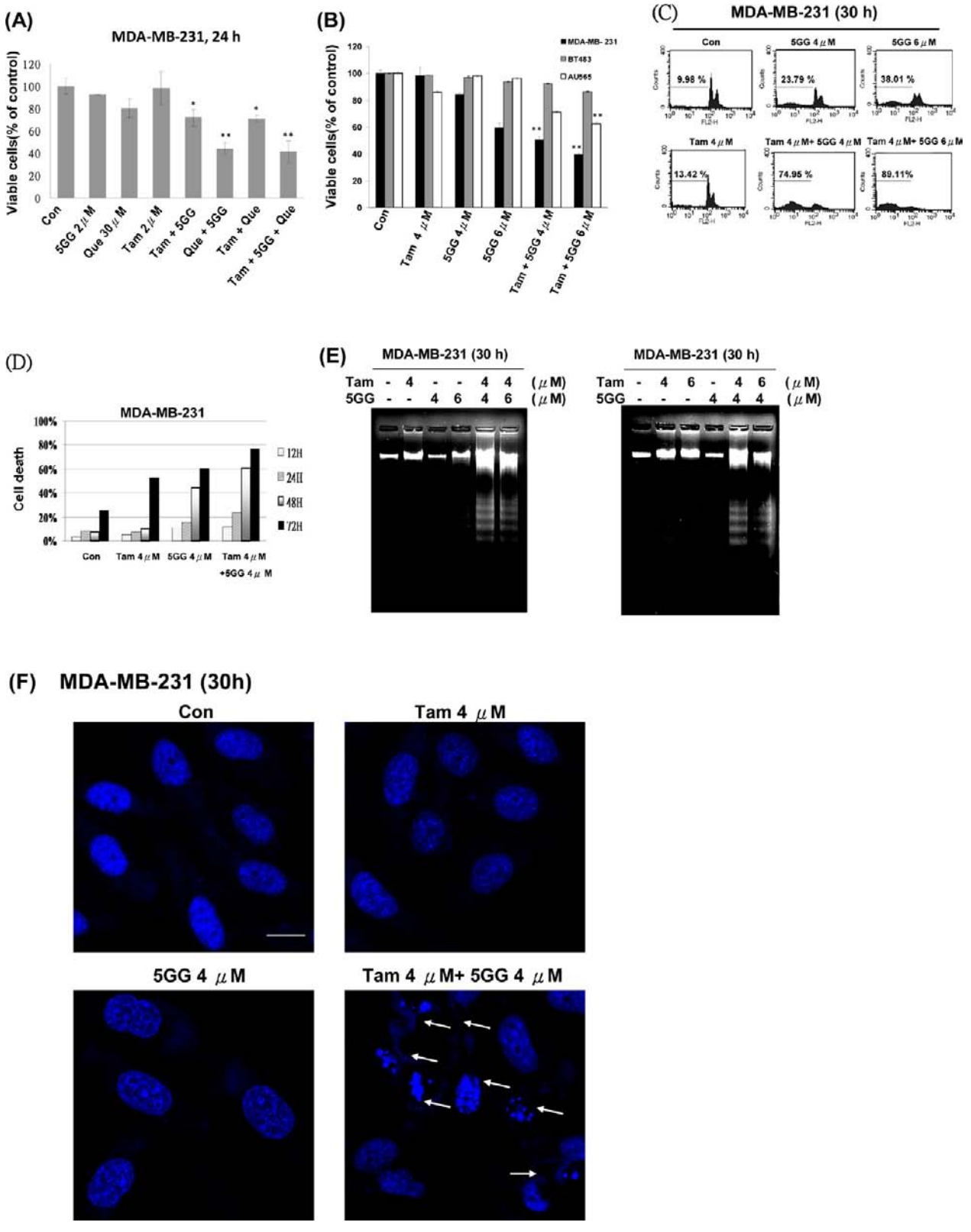


**Figure 9.** continued


dx.doi.org/10.1021/jf305253m | J. Agric. Food Chem. 2013, 61, 6430−6445

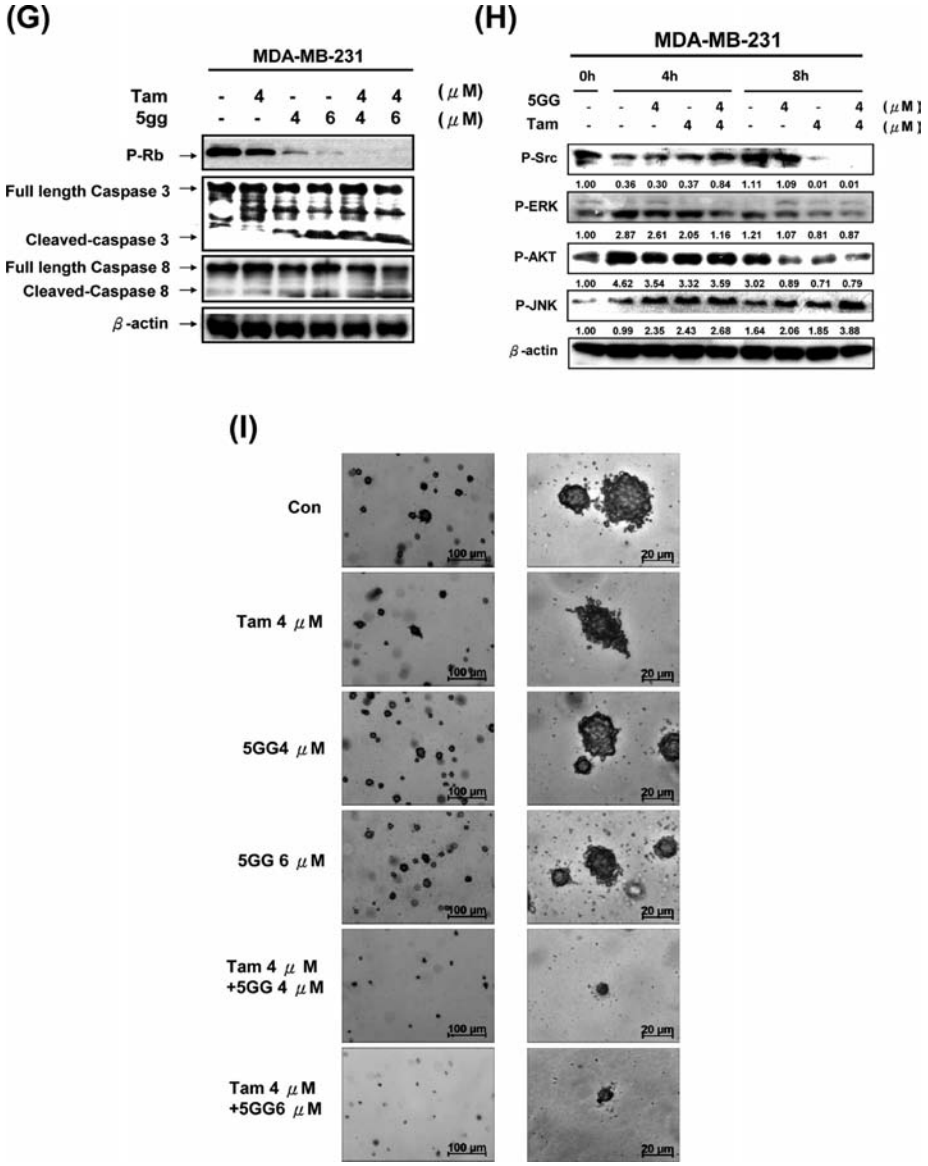


**Figure 9.** Effects of co-treatment with tamoxifen plus 5GG and tamoxifen plus Que on proliferation of breast cancer cells. (A, B) Cells were cultured in DMEM supplemented with 10% fetal calf serum for 24 h. After culturing for 24 h, cells were treated with DMSO, Que, 5GG, tamoxifen, and a combination of Que, 5GG, and tamoxifen, respectively. Cell growth inhibition was determined by MTT assay. The number of viable cells after treatment is expressed as a percentage of the vehicle-only control. Data are the mean ± SE of three independent experiments. Co-treatment was more effective than treatment with either agent alone: *, $p < 0.05$; **, $p < 0.01$; ***, $p < 0.001$ by ANOVA followed by Dunnett's multiple comparison test. (C) Changes in cell cycle phase distribution following co-treatment with tamoxifen plus 5GG were examined using flow cytometry. The cytotoxic effect on MDA-MB-231 cells co-treated with tamoxifen plus 5GG was examined using the trypan blue exclusion assay (D), DNA fragmentation assay (E), and Hochest assay (F) as described in the Materials and Methods section. Induction of caspase activation (G) and inhibition of Src, ERK1/2, AKT phosphorylation (H) in MDA-MB-231 cells co-treated with tamoxifen plus 5GG. The values below the figures represent changes in protein level of the bands normalized to 0 h-treated control. (I) Effect of co-treatment with tamoxifen plus 5GG on colony formation in MDA-MB-231 cells was determined using the soft agar colony formation assay.

**Caspase Activity.** Tamoxifen, an estrogen analogue, is a very effective agent used in the treatment of breast cancer patients. Next, we tested the effect of co-treatment with tamoxifen, 5GG, and Que on MDA-MB-231 cells. It was found that 5GG combined with Que was more effective in inhibiting MDA-MB-231 cell growth compared with tamoxifen combined with 5GG or Que (Figure 9A).

It is well known that Que could enhance the growth inhibitory ability of tamoxifen.[35] However, the combined effect of tamoxifen and 5GG has not been reported previously. In this study, the combined effect of tamoxifen and 5GG on MDA-MB-231, AU565, and BT483 cells was evaluated using the MTT assay. Co-treatment with 4 μM tamoxifen plus 4 μM 5GG for 30 h synergistically reduced cell growth in MDA-MB-231 and AU565 cells, but not in BT483 cells (Figure 9B). In MDA-MB-231 cells, the sub-G1 phase of cells co-treated with 4 μM tamoxifen and 4 μM 5GG was elevated by 41.16% and 59.53%, as compared with that of cells treated using 4 μM tamoxifen and 4 μM 5GG alone, respectively (Figure 9C). These results demonstrate that tamoxifen and 5GG act synergistically to induce apoptosis, but not cell cycle arrest, in MDA-MB-231 cells. Next, we determined the synergistic

cytotoxic effect of co-treatment with tamoxifen plus 5GG in MDA-MB-231 cells using the trypan blue exclusion assay, DNA fragmentation assay, and Hochest assay. Treatment of MDA-MB-231 cells with 4 $\mu$M tamoxifen or 4 $\mu$M 5GG alone induced cell death by 9.1% or 42.3% at 48 h and 56.1% or 60.1% at 72 h, respectively. Compared with that induced by tamoxifen and 5GG alone, cell death induced by co-treatment with tamoxifen plus 5GG in MDA-MB-231 cells was enhanced by 61.5% at 48 h and 78.8% at 72 h (Figure 9D). In addition, treatment of MDA-MB-231 cells with tamoxifen or 5GG alone did not induce DNA fragmentation. However, co-treatment with tamoxifen plus 5GG induced dose-dependent DNA fragmentation (Figure 9E). The induction of apoptosis by co-treatment with tamoxifen plus 5GG in MDA-MB-231 cells was further confirmed in fluorescence photomicrographs of cells stained with Hoechst 33258 after 30 h co-treatment. The control cells showed round and homogeneous nuclei, whereas cells co-treated with tamoxifen plus 5GG showed condensed and fragmented nuclei (arrows) (Figure 9F). These results demonstrate that tamoxifen and 5GG act synergistically to induce cell death and DNA fragmentation in MDA-MB-231 cells.

To identify the underlying molecular mechanism of the synergy between tamoxifen and 5GG, Western blot analysis was performed to profile the expression of apoptosis regulatory proteins in MDA-MB-231 cells treated with a single agent and combination therapy. Figure 9G shows that co-treatment with tamoxifen plus 5GG decreased full-length caspase 3, full-length caspase 8, and P-RB, but increased cleaved caspase 3 and cleaved caspase 8 in MDA-MB-231 cells. Next, we explored the underlying signal transduction pathways of tamoxifen plus 5GG-induced apoptosis. We determined the combined effect of tamoxifen and 5GG under different treatments during 4−8 h on the actions of Src, ERK1/2, AKT, and JNK. Figure 9H shows that the phosphorylation of Src, ERK1/2, and AKT in MDA-MB-231 cells co-treated with tamoxifen plus 5GG at 8 h was synergistically reduced, but the phosphorylation of JNK was synergistically increased.

To determine cell anchorage-independent proliferation potential, MDA-MB-231 cells co-treated with tamoxifen and 5GG were plated in soft agar for six weeks. After six weeks in the cultures, co-treatment with tamoxifen plus 5GG synergistically reduced the capacity for soft agar colony formation (Figure 9I).

## 4. DISCUSSION

Several clinical studies have used natural dietary compounds containing a mixture of various phytochemicals for human cancer prevention;[36,37] hence, it is important to investigate their combined effect. To our knowledge, this work is the first study on the different mechanisms involved in cell cycle arrest and apoptosis induced by Que combined with 5GG in MDA-MB-231 and AU565 cells (Figure 10). We found that Que combined with 5GG can synergistically decrease SKP2 in MDA-MB-231 cells (ER-/Her2-negative, SKP2-overexpressing breast cancer cell lines), but decreases Her2 in AU565 cells (ER-negative/Her2-positive breast cancer cell lines). A recent study found that SKP2 upregulation is strongly correlated with Akt activation and promotion of tumor progression in Her2-positive breast cancer patients.[38] In the present study, 5GG and Que also synergistically suppressed cell proliferation in MDA-MB-231.eB cells (SKP2/Her2-overexpressing cell line) through downregulation of SKP2 and Her2 protein. Our results suggest

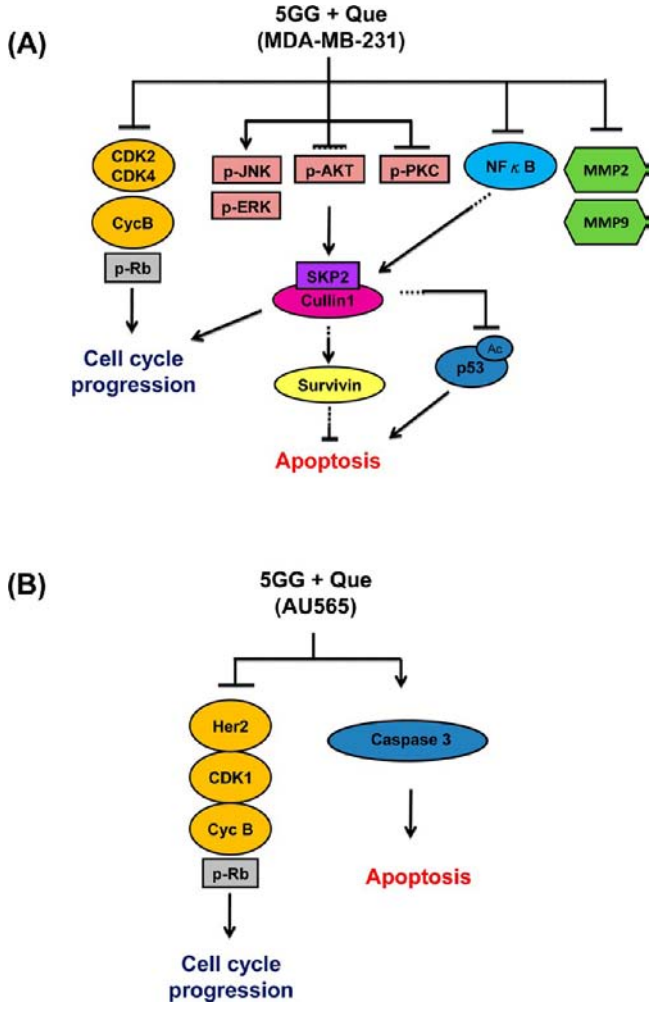


**Figure 10.** Diagram illustrating the action of combination with Que and 5GG in regulating cell cycle arrest and apoptosis in MDA-MB-231 (A) and AU565 (B) cells.

that 5GG combined with Que proved exceedingly effective for the development of potent antibreast cancer agents that can pharmacologically target both SKP2 and Her2. Similar results have been found in other studies. Altenburg et al. reported that DHA enhancement of cellular curcumin uptake is an important mechanism in anticancer activity.[39] Another study pointed out that the combination of resveratrol, Que, and catechin significantly reduced cancer cell growth *in vitro*.[5] We also found that 5GG in combination with kaempferol, apigenin, or luteolin had a synergistic effect on MDA-MB-231 cells (data not shown).

Wang et al. reported that 50% EGCG was present in methylated form (4′-MeEGCG) in human and mouse tissue.[40,41] Methylation decreased the EGCG bioactivity, and it was excreted in the urine. Que, a catechol-*O*-methyl transferase (COMT) inhibitor, was known to inhibit EGCG methylation. Additionally, Que combined with EGCG synergistically reduced cancer cell growth and decreased EGCG methylation. 5GG contains five gallate moieties and is structurally similar to EGCG, which contains one gallate moiety. We evaluated the ability of Que combined with 5GG, EGCG, and GA, respectively, to reduce MDA-MB231 cell growth. The decrease in efficiency was on the order of 5GG > EGCG > GA, suggesting that the presence of a gallate moiety


dx.doi.org/10.1021/jf305253m | *J. Agric. Food Chem.* 2013, 61, 6430−6445

could enhance the growth inhibitory ability of Que. Our findings are consistent with previous results that the gallate moiety is required for antiproliferative effects in human colon adenocarcinoma cells.[21] However, the issue of whether 5GG would be methylated by COMT in human tissue or whether Que could decrease 5GG methylation to enhance the biological effect of 5GG needs further study.

After SKP2 knockdown in MDA-MB-231 cells, we also observed repression of cullin 1, CDK2, and survivin, but upregulation of cleavage caspase 3 and acetyl-p53. The findings of the current study are consistent with recent research demonstrating that downregulation of SKP2 using siRNA increased p53- and caspase3-dependent apoptosis[34] and decreased CDK2-mediated cell cycle progression.[28] Therefore, these results suggest that cell cycle arrest and apoptosis are induced through the suppression of the SKP2 pathway. The actual role of SKP2 in apoptosis and growth inhibition remains unclear, which merits further research. Kitagawa et al. reported that SKP2 suppresses p300-mediated acetylation of p53 (Lys 382) and the transactivation ability of p53.[34] Our results also found that 5GG combined with Que synergistically increased p53 and acetyl-p53 (Lys382) protein levels in a time-dependent manner. The issue of whether or not the SKP2/P300 pathway is a direct target for co-treatment with 5GG plus Que needs further study.

Tamoxifen is the oldest and the most commonly prescribed selective estrogen-receptor modulator. However, five-year tamoxifen use has become associated with a number of serious side effects.[42] Therefore, alternative interventions are needed to replace or to supplement current regimens. In the current study, tamoxifen in combination with 5GG or Que had a synergistic effect in MDA-MB-231 cells. However, co-treatment with 2 $\mu$M 5GG plus 30 $\mu$M Que was more effective than co-treatment with 2 $\mu$M tamoxifen plus 2 $\mu$M 5GG or 30 $\mu$M Que in reducing breast cancer cell growth. Because 5GG and Que are weak ER agonists/antagonists,[43] their combined effect was independent of their binding to ER and contributed to their superior synergized action. In addition, 5GG and Que were found to be less toxic than tamoxifen and had encouraging indications from epidemiology. Whether the co-treatment with 5GG plus Que can replace tamoxifen in breast cancer patients requires further investigation. On the other hand, the combination of tamoxifen and 5GG synergistically induced apoptosis, but not cell cycle arrest in MDA-MB-231 cells through caspase activity. It is also proposed that selective modification of Src, ERK1/2, and AKT inactivation probably contributes to the synergistic interaction. Taken together, our results point to 5GG as a suitable candidate for use in combination with cancer-preventive agents, such as tamoxifen, to reduce their adverse effects.

In conclusion, the combination of 5GG and Que can offer great potential for the chemoprevention of breast cancer, including SKP2 and Her2-positive breast cancer. These findings also offer additional insights into the induction of cell cycle arrest, apoptosis, and the inhibition of estrogen-independent growth in breast cancer cells by co-treatment with 5GG plus Que via direct downregulation of SKP2, Her2, and Akt signaling.

## AUTHOR INFORMATION


### Corresponding Author

*Tel: +886-3-5213132, ext. 2756. Fax: +886-3- 5257178. E-mail: jane@mail.nhcue.edu.tw.



### Funding

This work was supported by grants from the National Science Council, Taiwan (NSC 99-2320-B-134-001 and NSC 100-2313-B-134-001-MY3).


### Notes

The authors declare no competing financial interest.

## ABBREVIATIONS

5GG, 1,2,3,4,6-penta-*O*-galloyl-$\beta$-D-glucose; Her2, human epidermal growth factor receptor 2; Que, quercetin; SKP2, S-phase kinase protein 2

## REFERENCES


(1) Morabito, A.; Magnani, E.; Gion, M.; Sarmiento, R.; Capaccetti, B.; Longo, R.; Gattuso, D.; Gasparini, G. Prognostic and predictive indicators in operable breast cancer. *Clin. Breast Cancer* **2003**, *3* (6), 381−390.

(2) Signoretti, S.; Di Marcotullio, L.; Richardson, A.; Ramaswamy, S.; Isaac, B.; Rue, M.; Monti, F.; Loda, M.; Pagano, M. Oncogenic role of the ubiquitin ligase subunit Skp2 in human breast cancer. *J. Clin. Invest.* **2002**, *110* (5), 633−641.

(3) Olszewski, W. Clinical efficacy of micronized purified flavonoid fraction (MPFF) in edema. *Angiology* **2000**, *51* (1), 25−29.

(4) Walle, T.; Vincent, T. S.; Walle, U. K. Evidence of covalent binding of the dietary flavonoid quercetin to DNA and protein in human intestinal and hepatic cells. *Biochem. Pharmacol.* **2003**, *65* (10), 1603−1610.

(5) Schlachterman, A.; Valle, F.; Wall, K. M.; Azios, N. G.; Castillo, L.; Morell, L.; Washington, A. V.; Cubano, L. A.; Dharmawardhane, S. F. Combined resveratrol, quercetin, and catechin treatment reduces breast tumor growth in a nude mouse model. *Transl. Oncol.* **2008**, *1* (1), 19−27.

(6) Kim, Y. H.; Lee, D. H.; Jeong, J. H.; Guo, Z. S.; Lee, Y. J. Quercetin augments TRAIL-induced apoptotic death: involvement of the ERK signal transduction pathway. *Biochem. Pharmacol.* **2008**, *75* (10), 1946−1958.

(7) Ramos, A. M.; Aller, P. Quercetin decreases intracellular GSH content and potentiates the apoptotic action of the antileukemic drug arsenic trioxide in human leukemia cell lines. *Biochem. Pharmacol.* **2008**, *75* (10), 1912−1923.

(8) Wang, P.; Zhang, K.; Zhang, Q.; Mei, J.; Chen, C. J.; Feng, Z. Z.; Yu, D. H. Effects of quercetin on the apoptosis of the human gastric carcinoma cells. *Toxicol. in Vitro* **2011**, *26* (2), 221−228.

(9) Djuric, Z.; Severson, R. K.; Kato, I. Association of dietary quercetin with reduced risk of proximal colon cancer. *Nutr. Cancer* **2012**, *64* (3), 351−360.

(10) Hayashi, Y.; Matsushima, M.; Nakamura, T.; Shibasaki, M.; Hashimoto, N.; Imaizumi, K.; Shimokata, K.; Hasegawa, Y.; Kawabe, T. Quercetin protects against pulmonary oxidant stress via heme oxygenase-1 induction in lung epithelial cells. *Biochem. Biophys. Res. Commun.* **2012**, *417* (1), 169−174.

(11) Gibellini, L.; Pinti, M.; Nasi, M.; Montagna, J. P.; De Biasi, S.; Roat, E.; Bertoncelli, L.; Cooper, E. L.; Cossarizza, A. Quercetin and cancer chemoprevention. *Evid. Based Complementary Altern. Med.* **2011**, 591356.

(12) Staedler, D.; Idrizi, E.; Kenzaoui, B. H.; Juillerat-Jeanneret, L. Drug combinations with quercetin: doxorubicin plus quercetin in human breast cancer cells. *Cancer Chemother. Pharmacol.* **2011**, *68* (5), 1161−1172.

(13) Tang, S. N.; Singh, C.; Nall, D.; Meeker, D.; Shankar, S.; Srivastava, R. K. The dietary bioflavonoid quercetin synergizes with epigallocathechin gallate (EGCG) to inhibit prostate cancer stem cell characteristics, invasion, migration and epithelial-mesenchymal transition. *J. Mol. Signaling* **2010**, *5*, 14.

(14) Russo, M.; Spagnuolo, C.; Tedesco, I.; Bilotto, S.; Russo, G. L. The flavonoid quercetin in disease prevention and therapy: facts and fancies. *Biochem. Pharmacol.* **2012**, *83* (1), 6−15.

(15) Kwon, T. R.; Jeong, S. J.; Lee, H. J.; Sohn, E. J.; Jung, J. H.; Kim, J. H.; Jung, D. B.; Lu, J.; Kim, S. H. Reactive oxygen species-mediated activation of JNK and down-regulation of DAXX are critically involved in penta-O-galloyl-beta-d-glucose-induced apoptosis in chronic myeloid leukemia K562 cells. *Biochem. Biophys. Res. Commun.* **2012**, *424* (3), 530−537.
(16) Lee, H. J.; Seo, N. J.; Jeong, S. J.; Park, Y.; Jung, D. B.; Koh, W.; Lee, E. O.; Ahn, K. S.; Lu, J.; Kim, S. H. Oral administration of penta-O-galloyl-beta-D-glucose suppresses triple-negative breast cancer xenograft growth and metastasis in strong association with JAK1-STAT3 inhibition. *Carcinogenesis* **2011**, *32* (6), 804−811.
(17) Hu, H.; Zhang, J.; Lee, H. J.; Kim, S. H.; Lu, J. Penta-O-galloyl-beta-D-glucose induces S- and G(1)-cell cycle arrests in prostate cancer cells targeting DNA replication and cyclin D1. *Carcinogenesis* **2009**, *30* (5), 818−823.
(18) Ryu, H. G.; Jeong, S. J.; Kwon, H. Y.; Lee, H. J.; Lee, E. O.; Lee, M. H.; Choi, S. H.; Ahn, K. S.; Kim, S. H. Penta-O-galloyl-beta-D-glucose attenuates cisplatin-induced nephrotoxicity via reactive oxygen species reduction in renal epithelial cells and enhances antitumor activity in Caki-2 renal cancer cells. *Toxicol. in Vitro* **2011**, *26* (2), 206−214.
(19) Shimizu, K.; Kamiya, O.; Hamajima, N.; Mizuno, H.; Kobayashi, M.; Hirabayashi, N.; Takeyama, H.; Kato, R.; Kawashima, K.; Nitta, M.; et al. Multi-drug combination therapy with vincristine-melphalan-cyclophosphamide-prednisolone was more effective than cyclophosphamide-prednisolone in stage III myeloma. The Nagoya Myeloma Cooperative Study Group. *Jpn. J. Cancer Res.* **1990**, *81* (12), 1320−1327.
(20) Kontoyiannis, D. P.; Lewis, R. E. Toward more effective antifungal therapy: the prospects of combination therapy. *Br. J. Hamaetol.* **2004**, *126* (2), 165−175.
(21) Salucci, M.; Stivala, L. A.; Maiani, G.; Bugianesi, R.; Vannini, V. Flavonoids uptake and their effect on cell cycle of human colon adenocarcinoma cells (Caco2). *Br. J. Cancer* **2002**, *86* (10), 1645−1651.
(22) Saijo, R.; Nonaka, G.; Nishioka, I. Tannins and related compounds. LXXXIV. Isolation and characterization of five new hydrolyzable tannins from the bark of Mallotus japonicus. *Chem. Pharm. Bull. (Tokyo)* **1989**, *37* (8), 2063−2070.
(23) Yu, D.; Jing, T.; Liu, B.; Yao, J.; Tan, M.; McDonnell, T. J.; Hung, M. C. Overexpression of ErbB2 blocks Taxol-induced apoptosis by upregulation of p21Cip1, which inhibits p34Cdc2 kinase. *Mol. Cell* **1998**, *2* (5), 581−591.
(24) Barre, B.; Perkins, N. D. The Skp2 promoter integrates signaling through the NF-kappaB, p53, and Akt/GSK3beta pathways to regulate autophagy and apoptosis. *Mol. Cell* **2010**, *38* (4), 524−538.
(25) Schneider, G.; Saur, D.; Siveke, J. T.; Fritsch, R.; Greten, F. R.; Schmid, R. M. IKKalpha controls p52/RelB at the skp2 gene promoter to regulate G1- to S-phase progression. *EMBO J.* **2006**, *25* (16), 3801−3812.
(26) Bashir, T.; Dorrello, N. V.; Amador, V.; Guardavaccaro, D.; Pagano, M. Control of the SCF(Skp2-Cks1) ubiquitin ligase by the APC/C(Cdh1) ubiquitin ligase. *Nature* **2004**, *428* (6979), 190−193.
(27) Muth, D.; Ghazaryan, S.; Eckerle, I.; Beckett, E.; Pohler, C.; Batzler, J.; Beisel, C.; Gogolin, S.; Fischer, M.; Henrich, K. O.; Ehemann, V.; Gillespie, P.; Schwab, M.; Westermann, F. Transcriptional repression of SKP2 is impaired in MYCN-amplified neuroblastoma. *Cancer Res.* **2010**, *70* (9), 3791−3802.
(28) Shin, J. S.; Hong, S. W.; Lee, S. L.; Kim, T. H.; Park, I. C.; An, S. K.; Lee, W. K.; Lim, J. S.; Kim, K. I.; Yang, Y.; Lee, S. S.; Jin, D. H.; Lee, M. S. Serum starvation induces G1 arrest through suppression of Skp2-CDK2 and CDK4 in SK-OV-3 cells. *Int. J. Oncol.* **2008**, *32* (2), 435−439.
(29) Nicolini, A.; Giardino, R.; Carpi, A.; Ferrari, P.; Anselmi, L.; Colosimo, S.; Conte, M.; Fini, M.; Giavaresi, G.; Berti, P.; Miccoli, P. Metastatic breast cancer: an updating. *Biomed. Pharmacother.* **2006**, *60* (9), 548−556.
(30) Lin, H. K.; Chen, Z.; Wang, G.; Nardella, C.; Lee, S. W.; Chan, C. H.; Yang, W. L.; Wang, J.; Egia, A.; Nakayama, K. I.; Cordon-Cardo, C.; Teruya-Feldstein, J.; Pandolfi, P. P. Skp2 targeting suppresses tumorigenesis by Arf-p53-independent cellular senescence. *Nature* **2010**, *464* (7287), 374−379.
(31) Yokoi, S.; Yasui, K.; Mori, M.; Iizasa, T.; Fujisawa, T.; Inazawa, J. Amplification and overexpression of SKP2 are associated with metastasis of non-small-cell lung cancers to lymph nodes. *Am. J. Pathol.* **2004**, *165* (1), 175−180.
(32) Hung, W. C.; Tseng, W. L.; Shiea, J.; Chang, H. C. Skp2 overexpression increases the expression of MMP-2 and MMP-9 and invasion of lung cancer cells. *Cancer Lett.* **2010**, *288* (2), 156−161.
(33) Hu, R.; Aplin, A. E. Skp2 regulates G2/M progression in a p53-dependent manner. *Mol. Biol. Cell* **2008**, *19* (11), 4602−4610.
(34) Kitagawa, M.; Lee, S. H.; McCormick, F. Skp2 suppresses p53-dependent apoptosis by inhibiting p300. *Mol. Cell* **2008**, *29* (2), 217−231.
(35) Scambia, G.; Ranelletti, F. O.; Benedetti Panici, P.; Piantelli, M.; Bonanno, G.; De Vincenzo, R.; Ferrandina, G.; Pierelli, L.; Capelli, A.; Mancuso, S. Quercetin inhibits the growth of a multidrug-resistant estrogen-receptor-negative MCF-7 human breast-cancer cell line expressing type II estrogen-binding sites. *Cancer Chemother. Pharmacol.* **1991**, *28* (4), 255−258.
(36) Ghosh, N.; Ghosh, R.; Mandal, V.; Mandal, S. C. Recent advances in herbal medicine for treatment of liver diseases. *Pharm. Biol.***2011** *49* (9), 970−988.
(37) Greenwald, P. Clinical trials in cancer prevention: current results and perspectives for the future. *J. Nutr.* **2004**, *134* (12 Suppl), 3507S−3512S.
(38) Chan, C. H.; Li, C. F.; Yang, W. L.; Gao, Y.; Lee, S. W.; Feng, Z.; Huang, H. Y.; Tsai, K. K.; Flores, L. G.; Shao, Y.; Hazle, J. D.; Yu, D.; Wei, W.; Sarbassov, D.; Hung, M. C.; Nakayama, K. I.; Lin, H. K. The Skp2-SCF E3 ligase regulates Akt ubiquitination, glycolysis, herceptin sensitivity, and tumorigenesis. *Cell* **2012**, *149* (5), 1098−1111.
(39) Altenburg, J. D.; Bieberich, A. A.; Terry, C.; Harvey, K. A.; Vanhorn, J. F.; Xu, Z.; Jo Davisson, V.; Siddiqui, R. A. A synergistic antiproliferation effect of curcumin and docosahexaenoic acid in SK-BR-3 breast cancer cells: unique signaling not explained by the effects of either compound alone. *BMC Cancer* **2011**, *11*, 149.
(40) Wang, P.; Heber, D.; Henning, S. M. Quercetin increased bioavailability and decreased methylation of green tea polyphenols in vitro and in vivo. *Food Funct.* **2012**, *3* (6), 635−642.
(41) Wang, P.; Heber, D.; Henning, S. M. Quercetin increased the antiproliferative activity of green tea polyphenol (-)-epigallocatechin gallate in prostate cancer cells. *Nutr. Cancer* **2011**, *64* (4), 580−587.
(42) Nalepa, G.; Wade Harper, J. Therapeutic anti-cancer targets upstream of the proteasome. *Cancer Treat Rev.* **2003**, *29* (Suppl 1), 49−57.
(43) Mao, C.; Yang, Z. Y.; He, B. F.; Liu, S.; Zhou, J. H.; Luo, R. C.; Chen, Q.; Tang, J. L. Toremifene versus tamoxifen for advanced breast cancer. *Cochrane Database Syst. Rev.* **2012**, *7*, CD008926.
(44) Kumar, R.; Verma, V.; Jain, A.; Jain, R. K.; Maikhuri, J. P.; Gupta, G. Synergistic chemoprotective mechanisms of dietary phytoestrogens in a select combination against prostate cancer. *J. Nutr. Biochem.* **2011**, *22* (8), 723−731.